The Permeation of Methane Molecules through Silicalite-1 Surfaces[†]

Somphob Thompho,[‡] Rungroj Chanajaree,[‡,§] Tawun Remsungnen,[||] Supot Hannongbua,[§] Philippe A. Bopp,[⊥] and Siegfried Fritzsche*[,‡]

Institut für Theoretische Physik, Universität Leipzig, Vor dem Hospitaltore 1, D-04103 Leipzig, Germany, Department of Chemistry, Faculty of Science, Chulalongkorn University, Bangkok 10330, Thailand, Department of Mathematics, Faculty of Science, Khon Kaen University, Khon Kaen 40002, Thailand, and Department of Chemistry, Université Bordeaux 1, Building A12, 351 Cours de la Libération, F-33405 Talence CEDEX, France

Received: September 28, 2008; Revised Manuscript Received: December 20, 2008

The permeation of methane molecules through the silicalite-1 surfaces with and without silanol groups has been studied by nonequilibrium molecular dynamics computer simulations. A newly fitted intermolecular potential between the methane molecules and the silanol is used. A control volume provides a nearly stationary gas phase close to the membrane. The nonequilibrium process of filling the (initially empty) membrane with methane molecules until saturation is considered, and the surface permeability has been evaluated. It turns out to be strongly influenced by the presence of silanol groups. Additionally it was found that for a large part of the loading process the particle stream into the zeolite membrane was nearly independent upon the deviation from equilibrium. This means that far from equilibrium the decay of this deviation does not follow an exponential law.

1. Introduction

Investigations of nanoporous materials by computer simulations have been a field of research of rapidly growing interest during the last 30 years. This is due, on one hand, to the importance of these materials for many technical applications[1] and, on the other hand, to the progress in theoretical methods and computational power as well as to new experimental methods.[2,3]

While the transport of guest molecules within zeolites has been extensively examined during the last two decades[4,5] the investigation of effects at the external surface or in the transition region between gas phase and zeolite is still at its beginning. Nevertheless, this is an important subject as nanoporous materials are commonly used as powders, membranes, or hybrid materials. So, the penetration of the guest molecules through the external surface of zeolites is an essential step of their application and must be understood in detail.

Resistances of zeolite membranes against the flow of particles have recently been investigated in several simulations[6−15] and experimental papers.[16−18] To the best of our knowledge the influence of the silanol groups at the surface has been neglected throughout in the simulations of the surface resistance. However, adsorption processes may be influenced by these surface silanol.

For the present simulations, a slab is cut out as usual from an infinitely extended periodic membrane. Such a cut will leave unsaturated chemical bonds, which in reality are saturated by impurities or by hydrogen atoms forming silanol groups, as illustrated in Figure 1. In the above-mentioned papers the silanol groups are neglected and the same interaction parameters are used to describe the inside of the zeolite and its surface. Instead, in the present investigation we complete the cut bonds by silanol groups and determine from quantum mechanical calculations new interaction parameters between the methane molecules and the silanol groups. This includes the hydrogen atoms and those lattice oxygen atoms at the surface which are now connected with the hydrogen atoms forming the silanol groups.

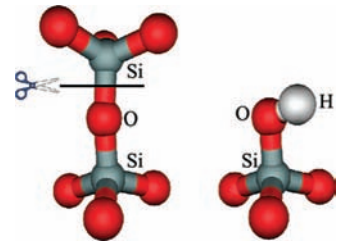

Figure 1. The silanol group completing a broken chemical bond.

2. The Model

In this paper we focus on the influence of the silanol groups, neglecting other effects connected with thin membranes.[14,15] Therefore, it is sufficient to use only a very thin membrane to separate the surface effects from other resistances against particle migration. Calculations with and without silanol groups have been performed on this system and the comparison of the results are at the core of this communication.

2.1. Quantum Fitted Intermolecular Potential between Methane and Silanol Surface. ***The Silanol Surface Model.*** The (010) external surface of silicalite-1, which is perpendicular to the straight channels, was selected. Surfaces with this orientation can be prepared experimentally in membranes.[19−22] They can also appear in naturally grown silicalite crystals.[23]

Potentials for the interaction of methane with the interior of the zeolite lattice are available in the literature. We decided to use the well-established MM2 parameters that we checked and

[†] Part of the special issue "Max Wolfsberg Festschrift".

* To whom correspondence should be addressed. E-mail: Siegfried.Fritzsche@uni-leipzig.de.
[‡] Universität Leipzig.
[§] Chulalongkorn University.
[||] Khon Kaen University.
[⊥] Université Bordeaux.

10.1021/jp808588n CCC: $40.75
Published on Web 02/10/2009

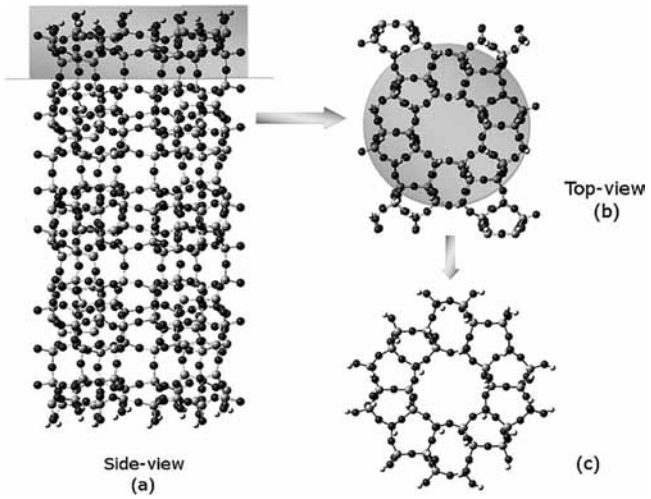

Figure 2. Side-view (a) and top-view (b) of the (010) surface, cut as indicated. After adding silanol (−OH) groups to the surface and energy minimization (for details see text) the obtained fragment (c) was used to represent the silanol covered (010) silicalite-1 surface in the quantum calculations.

used in earlier work.[24] In that model the lattice charges are taken into account implicitly by effective Lennard−Jones parameters. Potentials for the interaction of silanol with methane are available from generalized force fields like the DREIDING force field.[25] However, to avoid new fits for the interior of the zeolite and to use inside the zeolite the well-established parameters mentioned above, we needed, to be consistent, to employ an interaction model without explicit electric charges for the surface as well.

We thus had to find an appropriate "neutral" potential model for the methane/silanol interactions. The effect of the partial charges can be taken into account in the fitting procedure, at least at short enough distance. This should be sufficient in the case of the neutral methane for investigation of the surface effects.

Quantum-mechanical calculations by the ONIOM method[26] have been reported earlier[27−29] for the same system. Here we used previous quantum results[27−29] to develop for the present investigation a new neutral potential model for the surface/methane interaction.

The idealized MFI[30,31] crystal lattice shown in Figure 2a was chosen as starting structure in the quantum calculations for the silicalite-1 membrane. It was cut, as indicated in Figures 1 and 2. Then silanol groups were generated on the surface by adding hydrogen atoms to the oxygen dangling bonds. The chemical composition after this addition is $O_{86}Si_{32}H_{44}$. The positions of all hydrogen atoms were fully optimized using quantum chemical calculations at the HF/6-31G(d) level. The resulting optimized (rigid) surface fragment is shown in Figure 2c. It was used throughout for all quantum single-point energy calculations.

Development of the Methane Silanol Surface Potential Functions. Numerous complexes between a rigid methane molecule and the frozen optimized silanol surface have been generated by varying the orientation of the methane molecule and its distance from the surface at various points, as shown in Figure 3. The choice of points follows earlier work.[28] Subsequently, their (single-point) energies were obtained using ONIOM (MP2/6-31G(d):HF/6-31G(d)) calculations with basis set superposition error (BSSE) correction.

ONIOM[26] is a method devised to enable the treatment of larger systems by introducing around a given molecule a small (so-called MODEL) region, which is treated with high accuracy, and a larger (so-called REAL) region, which is treated with lower accuracy to save computational effort.

The MODEL part and the REAL part for the ONIOM calculations[27−29] are shown in Figure 4. The MODEL part of the system has been treated quantum-mechanically with electronic correlations and the REAL part without these correlations.

The ONIOM interaction energy of the system, $\Delta E_{\mathrm{ONIOM}}$ can be estimated from three independent calculations as follows[26]

$$\Delta E_{\mathrm{ONIOM}} = E_{(\mathrm{REAL,LOW})} + E_{(\mathrm{MODEL,HIGH})} - E_{(\mathrm{MODEL,LOW})} \quad (1)$$

where $E_{(\mathrm{REAL,LOW})}$ is the total energy of the REAL system using the "low level" method, while $E_{(\mathrm{MODEL,HIGH})}$ and $E_{(\mathrm{MODEL,LOW})}$ denote the total energies of the MODEL part calculated with high and low level methods, respectively.

The methods of HF/6-31G(d) (called low level) and MP2/6-31G(d) (called high level) were applied to treat the REAL and the MODEL parts mentioned in eq 1. The GAUSSIAN03 package[32] was used for all calculations.

Then the coefficients of an analytical form $U(r)$ were fitted to the $\Delta E_{\mathrm{ONIOM}}$ of the complexes. This expression is a function of all distances from all methane sites to all the silanol surface sites shown in Figure 3

$$U(r) = \sum_{i}^{5} \sum_{j}^{162} -\frac{A_{ij}}{r_{ij}^{6}} + \frac{B_{ij}}{r_{ij}^{12}} + \frac{C_{ij}}{r_{ij}^{3}} \quad (2)$$

r denotes, summarily, all relevant coordinates; r_{ij} denotes the distance between site i of a methane molecule and site j of the surface fragment. We found in trials that this form provides the best-possible 3-term ansatz form fitting the total energies without explicit inclusion of a long-range electrostatic term.

Note that A_{ij}, B_{ij}, and C_{ij} are fitting parameters which are optimized to model the whole interaction between methane and silanol surface at once. Hence, a single parameter, taken separately, has no physical meaning. In particular, even the sign of a given coefficient can be different from one atom to the other. All fitted parameters as well as the ones used for the other parts of the membrane are summarized in Table 1.

We also simulate for comparison, with an identical setup, a membrane in which the hydrogen atoms of the silanol groups are ommitted and where the oxygen atoms at the surface are treated using the same interaction parameters as for all other oxygen atoms of the zeolite membrane (see section 4). This is the standard treatment in the literature that we propose here to modify.

2.2. Fit of the Potential values for Silanol−Methane. The ab initio method ONIOM(MP2/6-31G(d):HF/6-31G(d)) (see the very good introduction about the use of basis sets in the manual of ref 32) together with the appropriate BSSE corrections has been applied to investigate the interaction between the guest molecules methane (CH_4) and the (010) external surface of silicalite-1. The energies were generated for 250 configurations that differ in positions and orientations of the guest molecule with respect to surface.

The same positions as in ref 28 have been chosen. Only points at which the energies are less than 50 kJ were selected since the statistical weight of higher values is very low at the envisaged temperatures. Furthermore, including such high energies may bias the minimization of the sum of mean square deviations, resulting in an unsatisfactory representation of the really important regions around the minima of the potential energy surface.

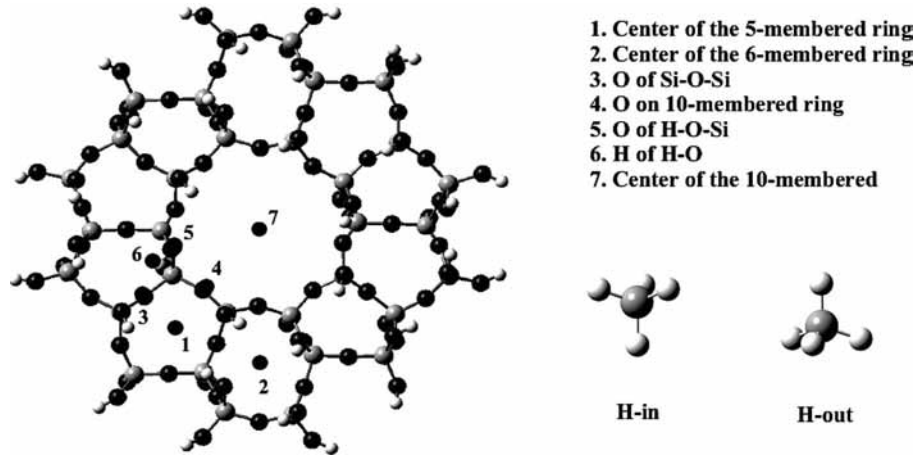

Figure 3. The methane molecule was located above and perpendicular to the points labeled as 1−7 in two configurations, H-in and H-out.

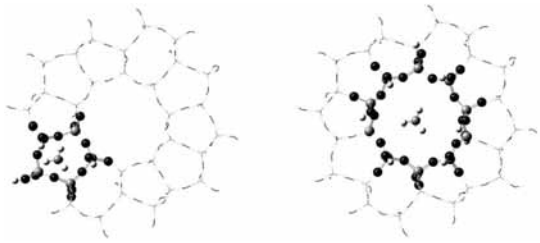

Figure 4. The MODEL part (drawn in ball-and-stick style) and the REAL part (whole picture, including the part only indicated by sticks), which were used in the ONIOM method. The left frame is for calculations 1 and 2 (in Figure 3); the right frame is for calculation 7 and the others.

TABLE 1: Potential Parameters for the Guest−Surface and the Guest−Zeolite Intermolecular Interaction[a]

i	j	A kJ/(mol·Å^6)	B kJ/(mol·Å^{12})	C kJ/(mol·Å^3)
Si_s	C	−141.60417	59597956.54480	−1857.28897
O_s	C	7541.98175	2578043.22354	1025.71435
H_s	C	−2377.64276	23141.74553	−610.83523
Si_s	H	2400.39670	160095.94649	353.86151
O_s	H	−1116.66782	32045.03425	−196.86810
H_s	H	134.37265	1199.90215	116.66330
Si_z	C	3644.84	8643900.0	
O_z	C	991.79	1070950.0	
Si_z	H	2050.69	2647470.0	
O_z	H	509.804	273789.0	

[a] Subscript s denotes surface, and subscript z denotes zeolite.

Fitting these energies ΔE_{ONIOM} by a multidimensional nonlinear least-squares procedure was possible with a function $U(r)$ consisting of a Lennard-Jones-type part and an additional inverse third power term, resulting in the expression given in eq 2. This expression is a function of all distances from all methane sites to all lattice atom sites of the cluster shown in Figure 4 for each case respectively.

The term B/r^{12} in eq 2 was constrained to be positive in order to avoid an unphysical negative singularity at short distances. We note that the r^{-6} term could not in all cases be forced to yield attraction like in the conventional Lennard-Jones potential.

An advantage of the present approach is that there is no additional fit to macroscopic measurements. A fit to macroscopic measurements would hopefully yield a correct reproduction of these macroscopic quantities but would be questionable for predicting microscopic properties. In our case the parameters are only fitted to the microscopic interaction energies obtained directly by the ab initio calculations.

To check the agreement between the fitted potential functions and the quantum calculations, Figures 5 and 6 show potential energy curves for various methane orientations. The correlation between ΔE_{ONIOM} and $U(r)$ is plotted in Figure 7 to illustrate the quality of the fit for various interaction energy ranges. It can be seen that the computed and fitted energies for methane/silicalite-1 are in good agreement, especially in the low-energy region, which plays the most important role for the molecular dynamics study.

2.3. The Silicalite-1 Flexible Lattice Model. The elasticity of the zeolite lattice is represented by the model of Demontis et al.,[33] which, besides harmonic terms, also includes an anharmonic term. For the O−H bond of the silanol group we use, according to Carte,[34] $f_r = 5124.8$ kJ/(mol·Å^2) and for the bond angle Si−O−H a force constant $f_w = 216.80$ kJ/(mol·rad^2).

For the rotation of the silanol hydrogen around the Si−O bond a 3-fold barrier of 3.27 kJ/mol has been found.[35] This weak barrier is neglected in many papers.[34] It is not straightforward to describe this torsional degree of freedom by an appropriate potential. The hydrogen of the silanol is located close to one corner (oxygen) of a tetrahedron and rotates around an axis defined by this corner and the center of the tetrahedron (silicon). Minima of the rotational potential occur when the projection of the hydrogen onto the plane of the remaining three corners (oxygen) of the tetrahedron is situated in the middle between the two adjacent oxygen.

One could define a dihedral angle (H−O−Si−O*) where O* is an arbitrarily chosen one among the three remaining corners of the tetrahedron. However, this will be unrealistic whenever, by rotation, the projection of the hydrogen is closer to another one of the three oxygens. This difficulty will be even more serious if, like here, the tetrahedron is flexible.

Therefore, we model the rotational elasticity by a soft repulsion in the plane of the three oxygen of the tetrahedron that do not belong to the silanol group between the projection of the hydrogen onto this plane and each one of these three oxygen. The bond angle Si−O−H is perpendicular to this plane and will not be much influenced by this repulsion. Additionally, this repulsion is such that the small component of the force in direction of the O−H bond is negligible compared to the average forces originating in the harmonic terms. The surface is essentially parallel to the xz plane, see Figure 8.

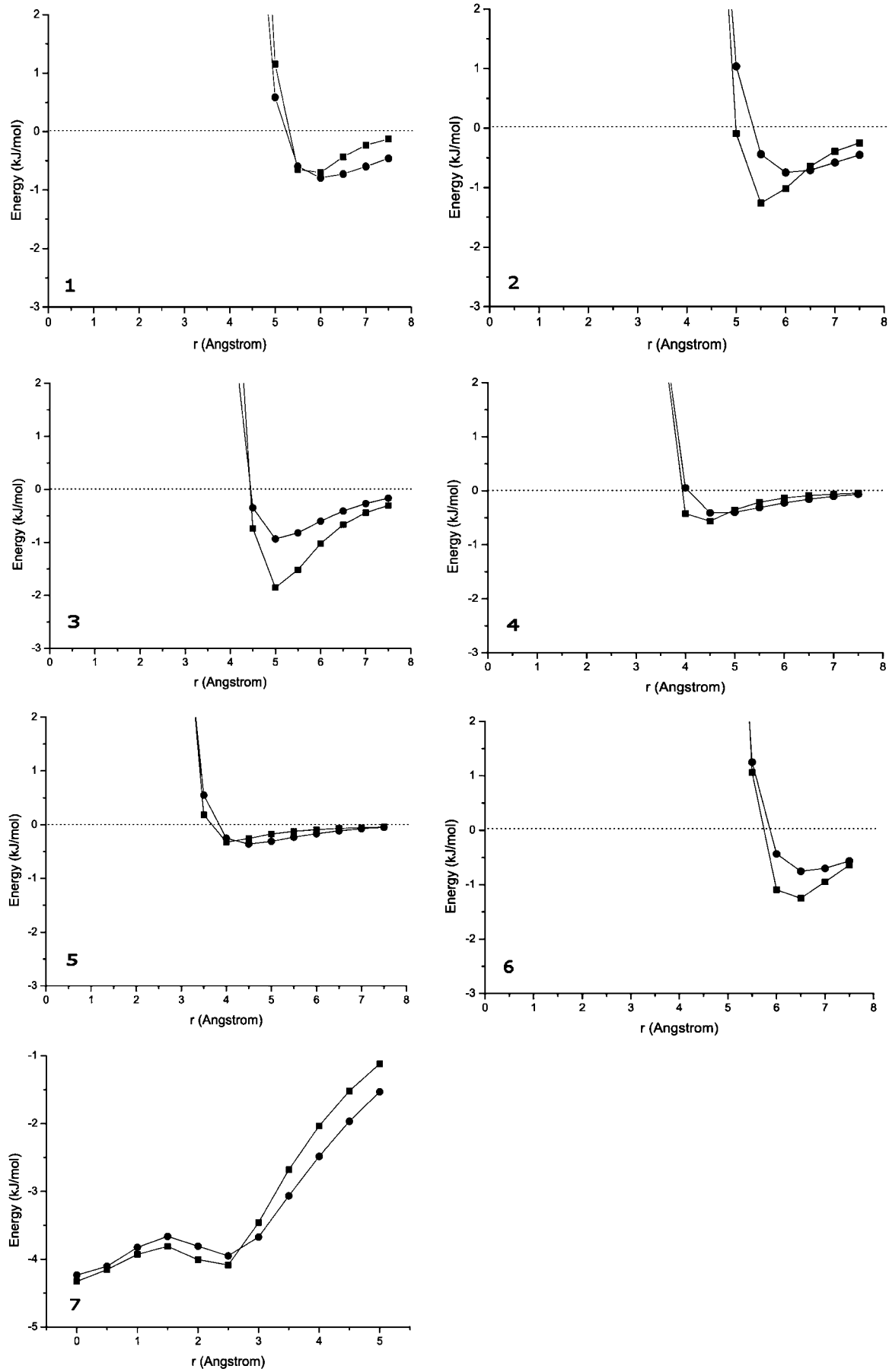

Figure 5. Methane/silicalite-1 interaction energies obtained from the ONIOM method (squares) and the fitted potential, according to eq 2 (circles) using the fitted parameters summarized in Table 1. Labels 1−7 denote the methane trajectories 1−7 defined in Figure 3 with methane in the H-in configuration. The interatomic distances are between the C atom of methane and atoms 1−7 or the center of the ring.

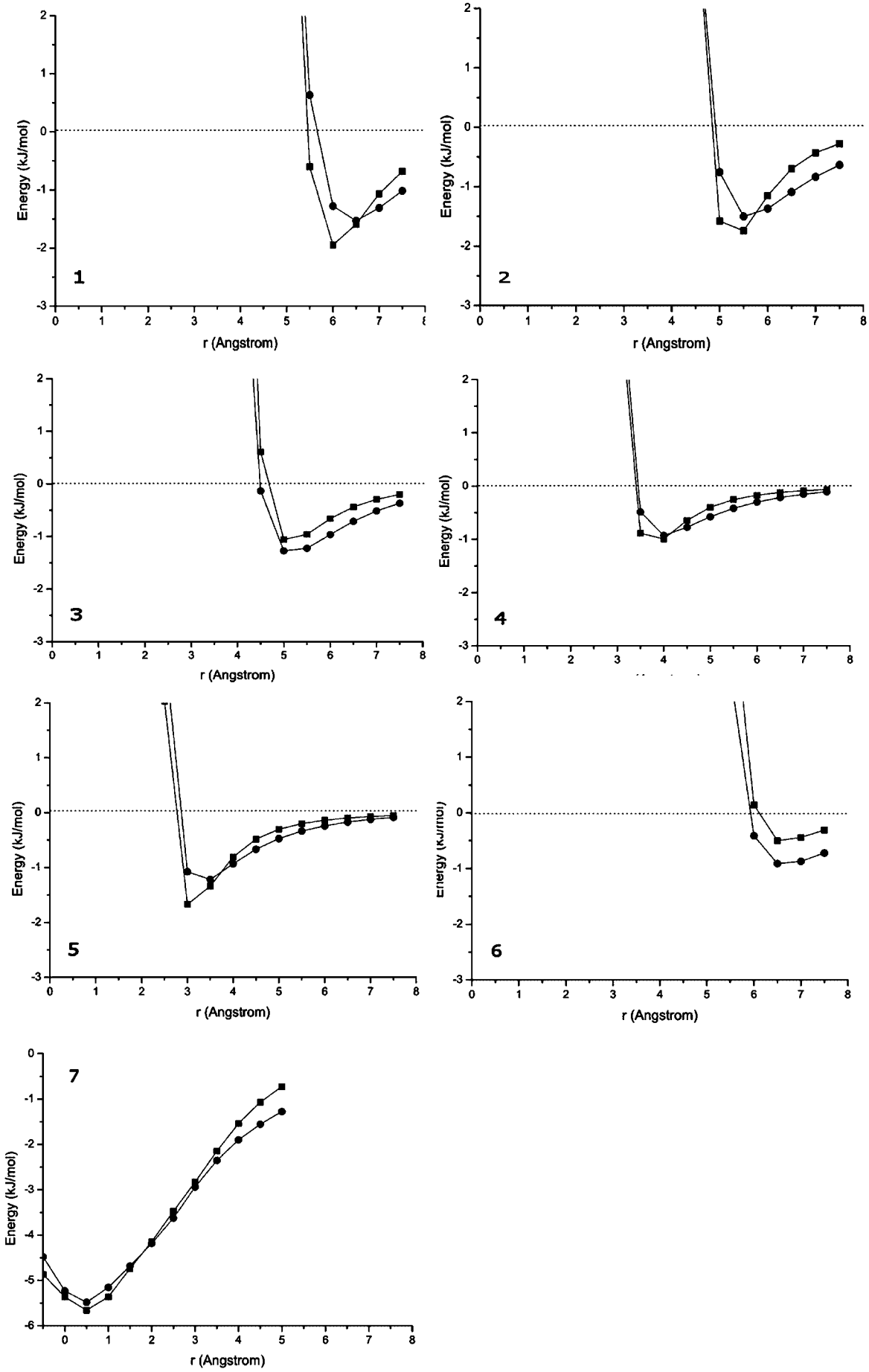

Figure 6. Methane/silicalite-1 interaction energies for H-out configuration obtained from the ONIOM method (square) and fitted potential (circles) as in Figure 5.

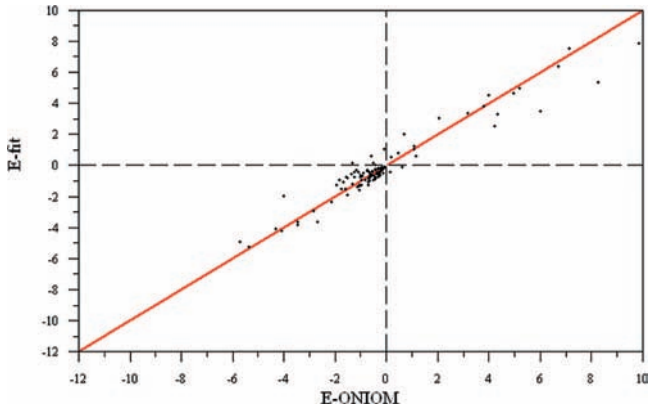

Figure 7. A correlation plot comparing potential energy values calculated from the fitted potential function (eq 2) with ab initio values. Each dot compares both values for one configuration. Energies in kJ/mol.

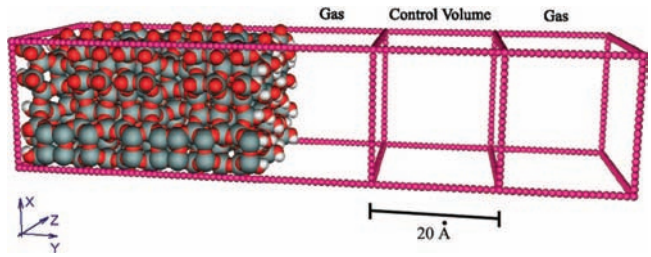

Figure 8. The simulation cell (MD box). Periodic boundary conditions are applied to this box in all directions.

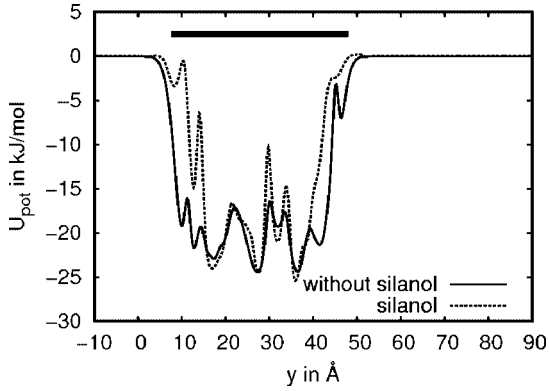

Figure 9. Plot of the potential experienced by a methane molecule moving along a central line within one of the channels of the membrane with and without silanol with fixed orientation. The orientation of the methane is such that three of its hydrogen form a plane parallel to the *xy* plane, one of them pointing in *y* direction. The black bar indicates which region is defined to be the interior of the membrane.

In calculation of the torsional potential we neglect small deviations from this orientation caused by the lattice vibrations. So the potential that we use is

$$U_{\mathrm{rot}} = \sum_{i=1}^{3} \frac{A}{r_{xz,i}^2}$$
$$r_{xz,i}^2 = [x(i) - x_{\mathrm{h}}]^2 + [z(i) - z_{\mathrm{h}}]^2 \qquad (3)$$

with $A = 2.0$ kJ/(mol·Å^2). The index i runs over the three oxygen atoms of the tetrahedron which are not connected with the hydrogen, and x_{h} and z_{h} are the x and z coordinates of the hydrogen.

To prevent a random drift of the whole membrane during the simulations as a consequence of the irregular collisions with the methane molecules an additional potential is added that yields a weak elastic bond between the center of mass of the lattice and its initial position. This tethering causes less perturbation to the system than the frequently used total fixing of one, or some, of the lattice atoms to their initial positions. For details see the supporting material.

2.4. Methane−Methane and Methane−Lattice Models. The harmonic valence force model of Bougeard and coworkers[36] is used for the internal degrees of freedom of the methane molecule.

The MM2 Lennard-Jones parameters of Burkert and Allinger[37] are used for the methane−methane and methane−lattice interactions. They yield the best results (compared to some others) for the thermodynamic and transport properties of methane in zeolites.[38] This was confirmed for the self-diffusion by our own tests.[24]

3. Description of the Stream and the Surface Permeability

Here we consider the nonequilibrium process of filling the initially empty membrane slab with methane molecules until saturation. We observe the time dependent particle stream into the zeolite membrane, $j = j(t)$. In agreement with previous studies,[17,18,39] we define the (time-dependent) surface permeability, $\alpha(t)$, by an ansatz that relates the flux to the concentration difference rather than to the difference in the pressure. This is done to avoid the difficulty of defining the pressure within the zeolite, e.g., as a virtual gas phase pressure. See also the discussion of this point in a previous work.[18] We feel encouraged to do so since it is easy to evaluate the local concentrations of the guest molecules in simulations and the local concentration is also accessible to new experimental techniques.[17,18,40] This common definition of α by eq 3 also allows to compare our results easily with literature ones. In agreement also with previous studies,[17,18,39] we thus define the surface permeability α by

$$\alpha(t) = \frac{j(t)}{c_{\mathrm{eq}} - c_{\mathrm{m}}(t)} \qquad (4)$$

$c_{\mathrm{m}}(t)$ is the concentration of guest molecules in a small region inside the porous solid close to the surface (called the marginal region throughout this paper, see below). c_{eq} is the equilibrium value of $c_{\mathrm{m}}(t)$. c_{eq} is a function of the gas phase density and of the temperature. The average number of particles adsorbed at the surface and other boundary effects[15] can also influence this quantity.

$j(t)$ is the stream, i.e., the number of particles that pass a surface of area A per area and per unit time

$$j = \frac{1}{A}\frac{\mathrm{d}N(t)}{\mathrm{d}t} \qquad (5)$$

For the case that the penetration into the straight y channel is examined, let A be two times the cross section of the MD simulation box in the xz plane, see Figure 8, because the membrane has two surfaces. Hence, $\Delta N/\Delta t$ is simply the change of the number of particles inside the membrane, in our simulation box, per unit time.

We note that it is not trivial to find an analytical ansatz for the functional dependence of the stream $j(t)$ upon the density difference $\Delta N(t) = c_{\mathrm{eq}} - c_{\mathrm{m}}(t)$.

4. The MD Simulations

4.1. Concept. Nonequilibrium molecular dynamics (NEMD) simulations have been carried out in which the adsorption process has been investigated. Starting with an empty zeolite

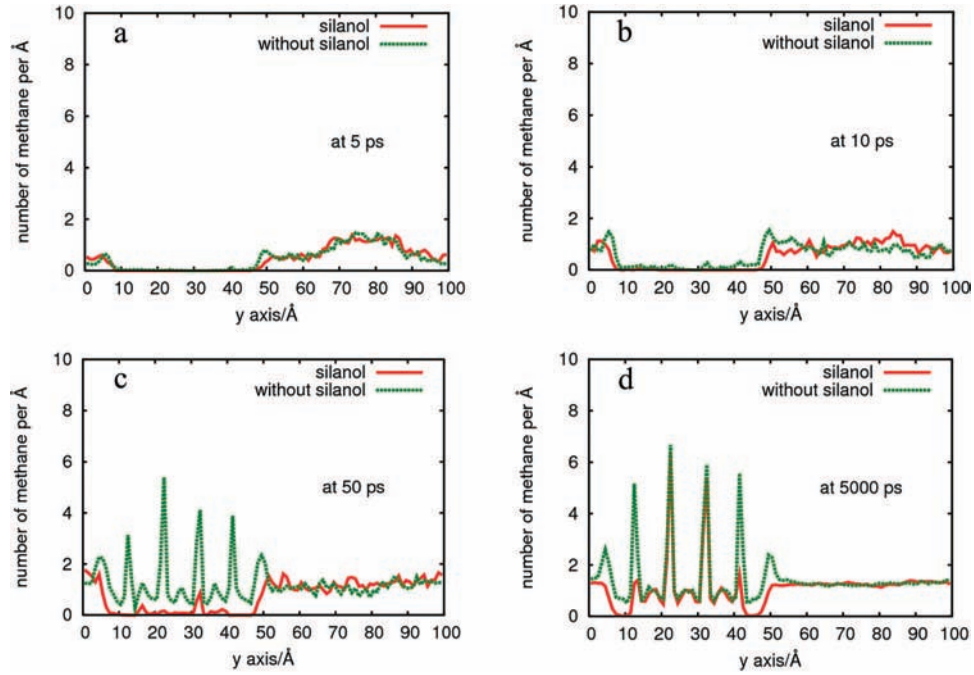

Figure 10. The density distribution along the *y* axis (see Figure 8) for the entire MD box as a function of time. The graphs are averages over the *xz* plane (see Figure 8) and over 10 nonequilibrium simulation runs at the given times.

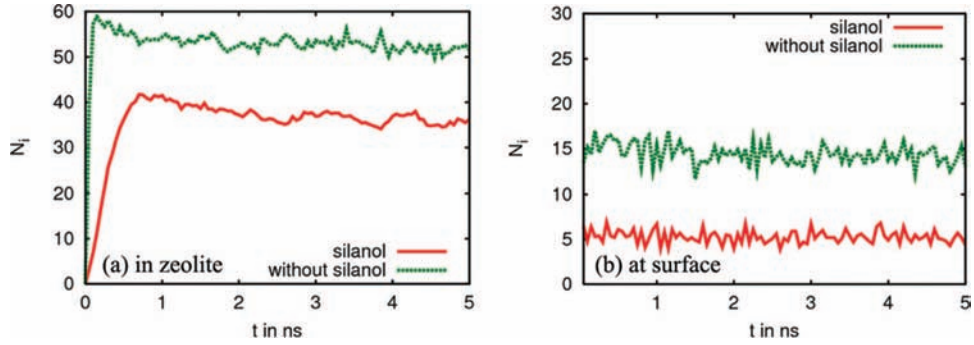

Figure 11. The number of particles adsorbed in the marginal zone of the zeolite, which is the whole interior of the zeolite in our case, and at its surface as a function of time.

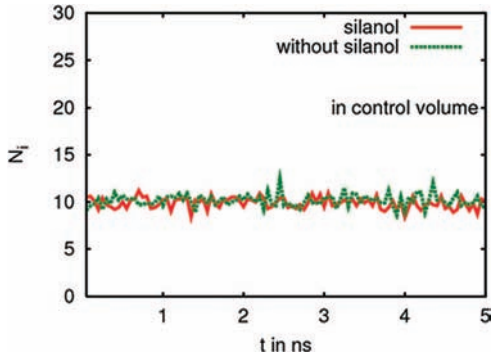

Figure 12. The number of methane molecules within the control volume.

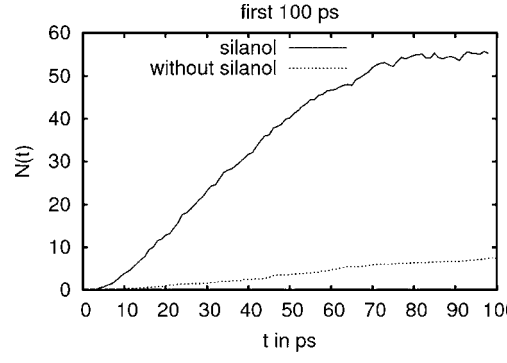

Figure 13. The first 100 ps of the adsorption process for both cases with/without silanol.

membrane and an empty gas phase (except for the control volume) the process of filling up the membrane is observed until equilibrium is reached.

Two cases are studied here: a membrane with silanol on the surface and a membrane without silanol.

Ten statistically independent MD runs are carried out in each case. They differ by the initial random distribution of particles in the control volume and by the sequence of random numbers that are used in the creation and removal of particles. Hence, they are microscopically different representations of the same macroscopic process. The concentrations as a function of time as well as all other time-dependent quantities are averaged over the ten statistically independent runs in order to reduce the statistical uncertainties in the results.

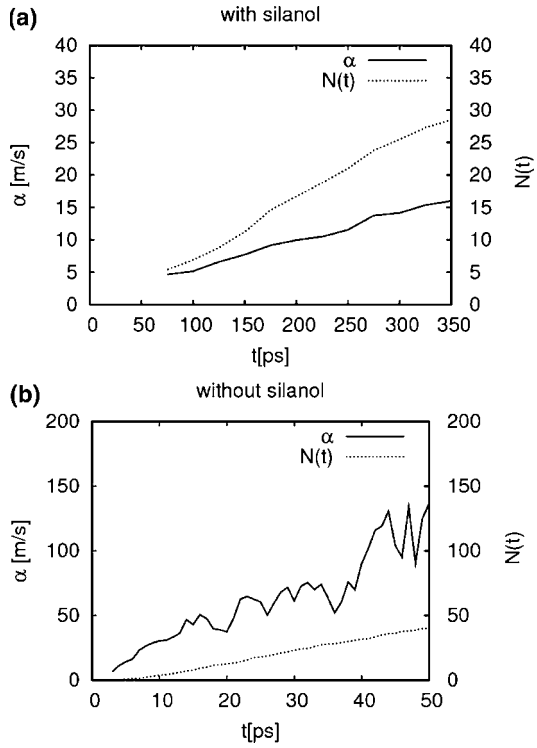

Figure 14. The surface permeability α with and without silanol groups. $N(t)$ is the number of methane within the membrane.

4.2. Grand Canonical MD in the Control Volume. To keep an approximately uniform gas phase in contact with the membrane throughout the adsorption process Grand Canonical MD (GCMD) is carried out.

Similar to a previous study,[41] we found that when using Grand Canonical Monte Carlo (GCMC) in the control volume the system was sensitive against the ratio of steps between stochastic MC moves in the bath region and MD steps for the whole system. Inhomogenities at the border between bath region and gas phase region appeared. Therefore, unlike the tests in ref 41, we totally omitted MC translation moves and we did only MD with randomly creating and deleting particles in the bath region. For more details see the supporting material.

In our simulations the particle movements are propagated by Newton's equation in the whole system, including the control volume.

As seen in Figure 10, a constant density distribution is established in the gas phase after about 5 ps, which is short compared to the time scale of the filling-up process of the zeolite. Plotting the trajectories shows that the methane molecules in the gas phase suffer collisions with each other and the surface of the membrane. They carry out a quasirandom walk in the gas phase before reaching the zeolite. Hence, the particles and, as a consequence the gas phase, are randomized effectively by such collisions in a natural way.

Note also that the bath region is about 20 Å away from the zeolite and that all our evaluations of the adsorption process focus only on the zeolite and its surface.

We examine the process of a gas cloud expanding from a source (one control volume) through the volume to the zeolite crystal and its penetration into the crystal. The object of our investigation is this nonsteady process itself and not the evaluation of the transport diffusion coefficient in an artificial steady state, which was critically discussed previously.[41] Instead, we ask if under these given conditions the same surface permeability α can be used for different times during the process of filling the zeolite, i.e., if a unique α for the whole process exists. This will turn out not to be the case.

Both effects, the sensitivity of the surface permeability with respect to the existence of silanol groups and the fact that an concentration independent surface permeability coefficient does not exist should not be affected by the streaming velocity in the way discussed previously.[41]

4.3. Technical Details of the MD Runs. The structure of the simulation cell is shown in Figure 8. It contains a zeolite lattice part, two gas regions, and a control volume in which methane molecules are created and removed according to a GC algorithm. The control volume is situated in the central part of the gas phase between 67 and 87 Å. Periodic boundary conditions are applied in all directions.

Figure 9 shows the potential profile for a single methane along a central line along one of the channels for the membrane with and without silanol. Note that the channel is not symmetric along a straight line. This is a consequence of the rotational symmetry of the membrane.

For each one of the two considered cases (with and without surface silanol), ten independent MD runs of 15,000,000 steps each have been carried out with a time step of 0.5×10^{-15} s for a total simulation time of 10 times 7.5 ns.

The control volume region, which is only a particle reservoir and not in direct interaction with the membrane or the gas near the surface, was kept at a constant temperature of 300 K by simple velocity rescaling. As the inserted particles start always with a velocity from the Boltzmann distribution belonging to the correct bath temperature only relatively small temperature differences have to be adjusted. The particle reservoir is of course not included in any evaluation of observables. All particles outside the control volume follow their Newtonian trajectories without any thermalization. The average concentration of 10 methane molecules inside the control volume corresponds to a pressure of about 34 MPa (according to the Van der Waals equation).

To examine the surface effects we have chosen the membrane thickness to be only two unit cells of silicalite, i.e., about 40 Å between the two surfaces. The largest possible distance to a surface is therefore about 20 Å. Thus, the complete interior of the membrane can be considered to form the marginal zone (see above) in our case. Hence, we have the concentration

$$c_{\mathrm{m}}(t) = \frac{2N(t)}{Ad} \tag{6}$$

where $N(t)$ is the number of guest molecules present at time t in the marginal zone and d is the depth of this marginal zone, which depends on the presence or absence of silanol. For our models we have $d = 38.67$ Å for the membrane with silanol groups and $d = 38.08$ Å for the case without silanol. This slight difference has only a minor quantitative influence on the values of α. Thus $\alpha(t)$ can be directly evaluated from

$$\alpha(t) = \frac{j(t)}{c_{\mathrm{eq}} - c_{\mathrm{m}}(t)} = \frac{d}{2[N_{\mathrm{eq}} - N(t)]}\frac{\mathrm{d}N(t)}{\mathrm{d}t} \tag{7}$$

5. Results and Discussion

The simulation started with an empty gas phase and empty zeolite. Soon after the start the methane density within the control volume reached a constant value and only random fluctuations around the stable average appeared throughout the run, as it should be in a GCMD system.

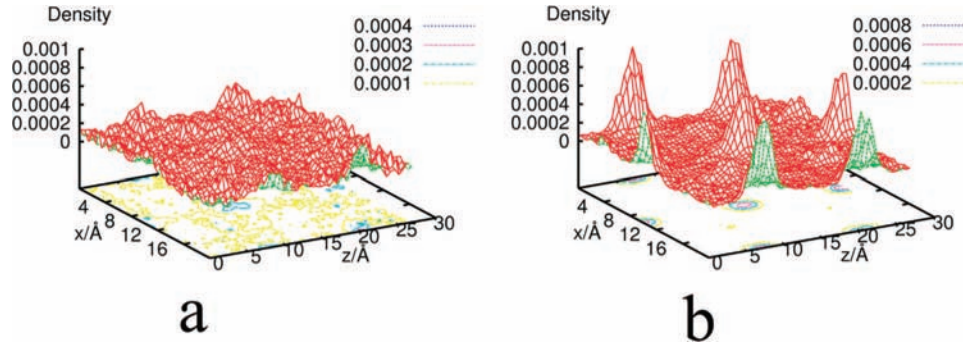

Figure 15. The normalized density distribution of methane at the surface in the final equilibrium state (a) with and (b) without silanol. Length is in angstroms.

Methane molecules quickly move out of control volume into the gas phase. The density distribution in the gas phase reaches its equilibrium after only about 10 ps, as seen in Figure 10. This figure also shows that the number of particles at the zeolite surface reaches its equilibrium value after about 50 ps.

Entering into and filling up the zeolite's marginal zone is a much slower process. This can be seen in Figure 11, which shows the long time development of the number of particles at the surface and in the marginal zone. The equilibrium in this zone is reached after times of the order of 0.1 ns for the system without silanol, and of approximately 1 ns for the system with silanol.

We note that the number of methane molecules inside the membrane exceeds the equilibrium number for a certain period of time. This period is about 0.1−2 ns in the case without silanol and 1−3 ns in the case with silanol. The reason for this nonequilibrium effect is not yet clear. Among other nonequilibrium effects it deserves a more detailed investigation in a forthcoming paper.

Figure 12 illustrates that the number of particles within the control volume, averaged over the 10 runs for one of our systems, is constant over time as mentioned above.

It is well-known that the process of migration of guest molecules within bulk zeolites has interesting energetic aspects.[24,42−45] Here, the presence of a gas phase and the adsorption process leads to even more complicated and interesting effects. The zeolite lattice is heated by the methane during the adsorption process because the potential energy of the methane within the zeolite is negative, while it is zero in the gas phase. A detailed analysis of this and other nonequilibrium effects such as energy redistribution will be subject of a forthcoming paper.

As an illustration of the dynamics of the particle stream Figure 13 shows the number of particles inside the zeolite for both cases for short times. $j(t)$ is the slope of this curve multiplied by a constant factor. $\Delta N(t)$, as defined above, is the difference between the particle number shown in Figure 13 and the equilibrium value N_{eq} ($N_{eq} = 51.53$ without silanol and $N_{eq} = 35.74$ with silanol). Obviously, $\Delta N(t)$ and $j(t)$ will both vanish in equilibrium.

If the decay of $\Delta N(t)$, which is the deviation of $N(t)$ from its equilibrium value, were exponential, the process should be described by an differential equation such as

$$\frac{d\Delta N(t)}{dt} = -k\Delta N(t) \tag{8}$$

with constant positive k. The solution of eq 8 would be

$$\Delta N(t) = \Delta N(0)\exp(-kt) \tag{9}$$

and $(d\Delta N(t))/(dt) = -(dN(t))/(dt)$ would never be constant except in the final equilibrium state where $\Delta N(\infty) = 0$. According to eq 5, one has $j(t) \propto (dN(t))/(dt)$. Therefore, k must be α times a constant factor, and hence, eq 8 with constant k corresponds to eq 4 with constant α.

A linear relation between $j(t)$ and $\Delta N(t)$, i.e., eq 4 with constant α will obviously be valid close to equilibrium, being the first nonvanishing term of a Taylor series of $j(t)$ as a function of $\Delta N(t)$. Thus, α as defined above will be constant in this limiting case.

Figure 13 shows that $\Delta N(t)$ is monotonically (except fluctuations) decreasing with time in both cases, with and without silanol. But, in contrast to this decay the slope $(dN(t))/(dt)$ in the case without silanol will first increase and then be nearly constant for the largest part of the process. Finally, it will decrease as it has to be. If silanol groups are present, the slope (hence also the stream) is nearly constant for the first 50 ps, although $\Delta N(t)$ is monotonically decreasing.

That means $j(t)$ will not depend on $\Delta N(t)$ during this time period in the case with silanol and it will also be constant in the case without silanol for the largest part of the relaxation process. The initial increase of the slope in the case without silanol may be connected with the high speed of the relaxation in this case and may be an artifact or special nonequilibrium effect. A constant stream while $\Delta N(t)$ is decreasing means that α as defined by eq 3 increases in time.

Figure 14 shows α from an early to an intermediate state of the adsorption process. For later times $\Delta N(t)$ becomes small, sometimes even zero, while its derivative is strongly fluctuating, even sometimes with alternating signs. In particular the fluctuations seen in the lower panel of Figure 14 are thought to be random. Therefore, reasonable results could not be obtained for later times. This would require drastically larger numbers of MD runs to be averaged.

It can clearly be seen that α is increasing with time. An α that increases with increasing loading (number of particles within the membrane) has also been found in previous work,[46] where the adsorption process has been investigated for a metal organic framework.

In ref 11, the surface resistance R is given, for methane at silicalite, as a function of the membrane thickness. R is the inverse of α. Extrapolating the curves shown in ref 11 to thin membranes, as considered here, gives values that are of the same order of magnitude as ours although the surface resistance is defined in ref 11 as being related to the gradient of p/k_BT, with p the pressure (k_B is Boltzmann's constant) rather than to the difference of concentrations as the surface resistance defined here. At low gas pressure, one has $n \approx p/k_BT$ in the constant volume, and the two definitions agree.

In contrast, the experimental values found for α of methane in a NaCaA zeolite[17,18] are 4 orders of magnitude smaller than ours. Therefore, additional surface resistances probably exist in the real system. Extra-framework cations that exist in NaCaA, but not in silicalite, may explain the large difference at least partially. The polarization interaction with neutral molecules can, e.g., reduce the self-diffusivity strongly.[47]

Figure 15 shows the spatial density distribution of adsorbed particles at the surface of the zeolite in the equilibrium state. It is normalized in such a way that the integral over the surface area yields a value of 1.0. It can clearly be seen that without silanol the density of the particles at the surface has higher values close to the channel mouths than in the other regions while with silanol the distribution is rather uniform.

6. Conclusions and Outlook

A neutral interaction model for the interaction of methane with the surface silanol groups has been developed. It was shown that the surface silanol groups have an considerable effect on the surface permeability and, hence, on the time scale of the adsorption process.

The surface permeability α has been shown to increase with increasing time, i.e., increasing number of guest molecules within the membrane. The reason for this effect is that the particle stream from the gas phase into the membrane is nearly constant over a large part of the adsorption process independently of the number of particles already adsorbed.

This fact should be a reason to think critically about the analytical ansatz for the time dependent macroscopic description of adsorption.

The MD program provides a nearly stationary gas phase and the adsorption process can be examined starting with an empty zeolite until saturation of the zeolite has been reached. This can be used in future for the examination of numerous nonequilibrium effects connected with the adsorption process.

Acknowledgment. We are grateful for the use of the computing facilities provided by the Computing Center of the Leipzig University, particularly for the technical help and support by Mr. Rost. P.A.B. thanks S.F. and S.H. for their hospitality during his visits. This work was financially supported by the Deutsche Forschungsgemeinschaft (DFG-FR1486/1-4) and the National Research Council of Thailand (NRCT, Grant No. GE 48/2547).

Supporting Information Available: Additional details are given in the Supporting Information material. This information is available free of charge via the Internet at http://pubs.acs.org.

References and Notes

(1) *Proceedings of the 15th International Zeolite Conference, Beijing, 12−17th August*, Elsevier: Amsterdam, 2007.

(2) Lehmann, E.; Vasenkov, S.; Kärger, J.; Zadrozna, G.; Kornatowskic, J. *J. Chem. Phys.* **2003**, *118*, 6129–6132.

(3) Heinke, L.; Chmelik, C.; Kortunov, P.; Shah, D. B.; Brandani, S.; Ruthven, D. M.; Kärger, J. *Microporous Mesoporous Mater.* **2007**, *104*, 18–25.

(4) Keil, F.; Krishna, R.; Coppens, M.-O. *Rev. Chem. Eng.* **2000**, *16*, 71–197.

(5) Haberlandt, R.; Fritzsche, S.; Vörtler, H. L. *Simulation of Microporous Systems: Confined Fluids in Equilibrium and Diffusion in Zeolites. In Handbook of Surfaces and Interfaces of Materials*; Nalwa, H. S., Ed.; Academic Press: San Diego, London, Boston, New York, Sidney, Tokyo, Toronto, 2001; Vol. 5, pp 358−444.

(6) Pohl, P.; Heffelfinger, G.; Smith, D. *Mol. Phys.* **1996**, *89*, 1725–1731.

(7) Martin, M. G.; Thompson, A. P.; Nenoff, T. M. *J. Chem. Phys.* **2001**, *114*, 7174–7181.

(8) Arya, G.; Maginn, E. J.; Chang, H. *J. Phys. Chem. B* **2001**, *105*, 2725–2735.

(9) Bowen, T. C.; Falconer, J. L.; Noble, R. D.; Skoulidas, A. I.; Sholl, D. S. *Ind. Eng. Chem. Res.* **2002**, *41*, 1641–1650.

(10) Ahunbay, M. G.; Elliott, J. R.; Talu, O. *J. Phys. Chem.* **2002**, *106*, 5163–5168.

(11) Ahunbay, M. G.; Elliott, J. R.; Talu, O. *J. Phys. Chem. B* **2004**, *108*, 7801–7808.

(12) Ahunbay, M. G.; Elliott, J. R.; Talu, O. *J. Phys. Chem. B* **2005**, *109*, 923–929.

(13) Newsome, D. A.; Sholl, D. S. *J. Phys. Chem. B* **2005**, *109*, 7237–7244.

(14) Gulin-Gonzalez, J.; Schüring, A.; Fritzsche, S.; Kärger, J.; Vasenkov, S. *Chem. Phys. Lett.* **2006**, *430*, 60–66.

(15) Vasenkov, S.; Schüring, A.; Fritzsche, S. *Langmuir* **2006**, *22*, 5728–5733.

(16) Jentys, A.; Tanaka, H.; Lercher, J. A. *J. Phys. Chem. B* **2005**, *109*, 2254–2261.

(17) Krutyeva, M.; Yang, X.; Vasenkov, S.; Kärger, J. *J. Magn. Reson.* **2007**, *185*, 300–307.

(18) Krutyeva, M.; Vasenkov, S.; Yang, X.; Caro, J.; Kärger, J. *Microporous Mesoporous Mater.* **2007**, *104*, 89–96.

(19) Engström, V. Ph.D. Thesis; Lulea University: Lulea, Sweden, 1999.

(20) Metzger, T. H.; Mintova, S.; Bein, T. *Microporous Mesoporous Mater.* **2001**, *43*, 191–200.

(21) Lai, Z.; Bonilla, G.; Diaz, I.; Nery, J.; Sujaoti, K.; Amat, M.; Kokkoli, E.; Terasaki, O.; Thompson, R.; Tsapatsis, M.; Vlachos, D. *Science* **2003**, *300*, 456–460.

(22) Zhang, F.; Fuji, M.; Takahashi, M. *J. Am. Ceram. Soc.* **2005**, *88*, 2307–2309.

(23) Roeffaers, M. B. J.; Ameloot, R.; Baruah, M.; Uji-i, H.; Bulut, M.; Cremer, G. D.; Müller, U.; Jacobs, P. A.; Hofkens, J.; Sels, B. F.; Vos, D. E. D. *J. Am. Chem. Soc.* **2008**, *000*, 000.

(24) Fritzsche, S.; Wolfsberg, M.; Haberlandt, R. *Chem. Phys.* **2003**, *289*, 321–333.

(25) Mayo, S. L.; Olafson, B. D. *J. Phys. Chem.* **1990**, *94*, 8897–8909.

(26) Morokuma, K. *Bull. Korean Chem. Soc.* **2003**, *24*, 797–801.

(27) Saengsawang, O.; Remsungnen, T.; Loisruangsina, A.; Fritzsche, S.; Haberlandt, R.; Hannongbua, S. *Stud. Surf. Sci. Catal.* **2005**, *158*, 947–954.

(28) Remsungnen, T.; Kormilets, V.; Loisruangsin, A.; Schüring, A.; Fritzsche, S.; Haberlandt, R.; Hannongbua, S. *J. Phys. Chem. B* **2006**, *110*, 11932–11935.

(29) Channajaree, R. *Adsorptions of Methane and Ethane Molecules on Silanol covered Silicalite-1 (010) Surface: Ab Initio fitted Potential*, Master Thesis; Chulalongkorn University: Bangkok, 2007.

(30) Caro, J.; M. Noack, M.; Kolsch, P.; Schafer, R. *Microporous Mesoporous Mater.* **2000**, *38*, 13–24.

(31) Baerlocher, Ch.; Meier, W. M.; Olson, D. H. *Atlas of Zeolite Framework Types*, 5th ed.; 2001.

(32) Frisch, M. J.; Trucks, G. W.; Schlegel, H. B.; Scuseria, G. E.; Robb, M. A.; Cheeseman, J. R.; Zakrzewski, V. G.; Montgomery, J. A., Jr.; Stratmann, R. E.; Burant, J. C.; Dapprich, S.; Millam, J. M.; Daniels, A. D.; Kudin, K. N.; Strain, M. C.; Farkas, O.; Tomasi, J.; Barone, V.; Cossi, M.; Cammi, R.; Mennucci, B.; Pomelli, C.; Adamo, C.; Clifford, S.; Ochterski, J.; Petersson, G. A.; Ayala, P. Y.; Cui, Q.; Morokuma, K.; Salvador, P.; Dannenberg, J. J.; Malick, D. K.; Rabuck, A. D.; Raghavachari, K.; Foresman, J. B.; Cioslowski, J.; Ortiz, J. V.; Baboul, A. G.; Stefanov, B. B.; Liu, G.; Liashenko, A.; Piskorz, P.; Komaromi, I.; Gomperts, R.; Martin, R. L.; Fox, D. J.; Keith, T.; Al-Laham, M. A.; Peng, C. Y.; Nanayakkara, A.; Challacombe, M.; Gill, P. M. W.; Johnson, B.; Chen, W.; Wong, M. W.; Andres, J. L.; Gonzalez, C.; Head-Gordon, M.; Replogle, E. S.; Pople, J. A. *Gaussian 03*, revision A.11; Gaussian, Inc.: Pittsburgh, PA, 2001.

(33) Demontis, P.; Suffritti, G. B.; Quartieri, S.; Fois, E. S.; Gamba, A. *J. Phys. Chem.* **1988**, *92*, 867–871.

(34) Carteret, C. *Spectrochim. Acta A* **2006**, *64*, 670–680.

(35) Abraham, R. J.; Grant, G. H. *J. Comput.-Aid. Mol. Des.* **1988**, *2*, 267–280.

(36) Dumont, D.; Bougeard, D. *Zeolites* **1995**, *15*, 650–655.

(37) Burkert, U.; Allinger, N. L. *Molecular Mechanics*; American Chemical Society: Washington D.C., 1982.

(38) Nicholas, J. B.; Trouw, F. R.; Mertz, J. E.; Iton, L. E.; Hopfinger, A. J. *J. Phys. Chem. B* **1993**, *97*, 4149–4163.

(39) Crank, J. *The Mathematics of Diffusion*; Clarendon Press: Oxford, 1975.

(40) Kärger, J.; Kortunov, P.; Vasenkov, S.; Heinke, L.; Shah, D. B.; Rakoczy, R. A.; Traa, Y.; Weitkamp, J. *Angew. Chem., Int. Ed.* **2006**, *45*, 7846–7849.

(41) Arya, G.; Chang, H.; Maginn, E. J. *J. Chem. Phys.* **2001**, *115*, 8112–8124.

(42) Fritzsche, S.; Haberlandt, R.; Kärger, J.; Pfeifer, H.; Wolfsberg, M. *Chem. Phys. Lett.* **1990**, *171*, 109–113.

(43) Fritzsche, S.; Wolfsberg, M.; Haberlandt, R.; Demontis, P.; Suffritti, G. B.; Tilocca, A. *Chem. Phys. Lett.* **1998**, *296*, 253–258.

(44) Fritzsche, S.; Wolfsberg, M.; Haberlandt, R. *Chem. Phys.* **2000**, *253*, 283–294.

(45) Fritzsche, S.; Haberlandt, R.; Schüring, A.; Wolfsberg, M. *The Mutual Influence of Dynamic Processes Acting in Different Time Scales. In Studies in Surface Science and Catalysis*; Galarneau, A., Renzo, F. D., Fajula, F., Vedrine, J., Eds.; Elsevier: Amsterdam, 2001; Vol. 106.

(46) Kortunov, P.; Heinke, L.; Arnold, M.; Nedellec, Y.; Jones, D. J.; Caro, J.; Kärger, J. *J. Am. Chem. Soc.* **2007**, *129*, 8041–8047.

(47) Fritzsche, S.; Haberlandt, R.; Kärger, J.; Pfeifer, H.; Heinzinger, K.; Wolfsberg, M. *Chem. Phys. Lett.* **1995**, *242*, 361–366.

JP808588N